REMOTE SENS. ENVIRON. 33:113–121 (1990)

On the Information Content of Soil Reflectance Spectra

John C. Price

Beltsville Agricultural Research Center, USDA

High resolution (.01 μm) reflectance spectra from more than 500 soils are analyzed to determine spectral variability in a portion of the visible and near infrared (0.55–2.32 μm), using a procedure previously developed for study of thermal infrared spectra. Four high spectral resolution basis vectors are sufficient to describe 99.6% of the spectral variability of the data set, with residual variability probably associated with the measurement process and instrument noise. Four broadband spectral measurements at .93–1.13 μm, 2.03–2.31 μm, .63–.74 μm, and 1.61–1.80 μm, together with a priori knowledge of the fitting vectors, are sufficient to describe the spectra of the soils studied.

INTRODUCTION

Although remote sensing studies of the earth's surface have been dominated by low spectral resolution measurements, such as the four broadband measurements of the Landsat Multispectral Scanners with bandwidths of .1 μm, .1 μm, .1 μm, and .3 μm, there has been continuing interest in higher spectral resolution measurements. Perforce such data implies more and more data points as the spectral region of interest, e.g., .4–2.5 μm in the visible and near infrared, is partitioned into finer and finer increments. In general, a computational problem results if the dimensionality of the measurements becomes too large, since standard methods for spectral analysis, such as principal components analysis, encounter difficulties. These problems result from two sources: First, the inversion of very high dimensionality matrices (e.g., 200×200) is computationally intensive and subject to roundoff errors, and, second, the existence of noise and spectral redundancy in the data studied can produce a tendency for matrix inversion to fail due to differencing and division by very small numbers. In this paper we study laboratory soil spectra obtained at the LARS laboratory facility (Stoner et al., 1980), having spectral resolution of .01 μm. These reflectance spectra with dimensionality $n = 178$ represent the range 0.55–2.32 μm. Using a procedure first developed for data in the thermal infrared with dimensionality $n = 862$ (Price, 1975), we show that the space of measurements for the 564 soils is spanned by four fitting functions or basis vectors, and that broadband measurements in four spectral intervals (.93–1.13 μm), (2.03–2.31 μm), (.63–.74 μm), and (1.61–1.80 μm), together with the known basis vectors, are sufficient to characterize the set of soil spectra. It follows that spectral discrimination of these soils must rely on at most four independent variables: Higher spectral resolution measurements provide redundant data. Thus the problem of soil classifi-

Address correspondence to John C. Price, USDA Agric. Res. Serv., Bldg. 1, BARC-West, Beltsville, MD 20705.

Received 9 April 1990; revised 17 July 1990.

0034-4257/90/$0.00

Published 1990 by Elsevier Science Publishing Co. Inc.

655 Avenue of the Americas, New York, NY 10010

cation from reflectance data is greatly simplified, while, at the same time, there is no need for additional high spectral resolution data for describing these spectra.

The next section presents the analysis procedure, which is more direct than that for thermal infrared spectra because effects of nonlinearity of the Planck function for emitted radiation may be avoided in reflectance spectra. The third section describes the LARS measurements and the result of application of the method to soil spectra. The last section summarizes the implications of the procedure, suggesting that, at least for soils, the value of additional high spectral resolution (.01 μm) measurements for soils is very limited.

PROCEDURE

The procedure used in this paper is a slightly modified version of that developed for study of spectra from the Infrared Interferometer Spectrometer (IRIS) on the Nimbus 4 satellite (Price, 1975). The IRIS instrument obtained spectra over the earth's surface in the spectral range 6.6–25 μm, with each spectrum represented by a set of 862 values. The description of statistical properties of such a high dimensionality measurement space requires special procedures, as any brute force method which calls for matrix inversion is clearly unacceptable. The method developed and employed is one of successive approximations, with the validity of the procedure determined by its convergence. For the soil spectra discussed later convergence is extremely rapid: Four spectral vectors represent the soils data sets to a residual error that may be ascribed to measurement error and to slight spectral variability, which may be associated with specific soils but is not statistically significant in the context of the data ensemble.

We seek a set of spectral basis functions which represent the spectral data set, and to find a set of broadband spectral intervals which are sufficient to determine uniquely the coefficients of these basis functions. The procedure is iterative: 1) We use the Gram–Schmidt procedure to select a limited set (10) of preliminary basis vectors which provide an approximation to the current version of the spectral data set. 2) We apply principal components analysis to the matrix resulting from the coefficients of these 10 basis vectors. Then from these low dimensionality eigenvectors plus the original basis vectors we may construct approximate eigenvectors for the full spectra. 3) From the first eigenvector, which describes most of the data set's variability, we select a spectral interval such that the wavelength integral of each sample spectrum may be used as a fitting variable to approximate the full spectrum. Then we compute this fitting function or basis vector. At the next iteration this fitting function is also to be subtracted from the original spectra, and the procedure is repeated by returning to step 1.

We indicate these steps formally.

Step 1. Let $x^\alpha = (x_1^\alpha, x_2^\alpha, \ldots, x_n^\alpha)$ represent a spectral measurement of dimensionality n, where the superscript α denoting the individual sample (in this case a soil spectrum) will frequently be deleted. We identify the inner product or dot product of two vectors y, z by

$$y^\alpha \cdot z^\beta = \sum_{i=1}^{n} y_i^\alpha z_i^\beta$$

and the norm by $|y| = [\Sigma y_k^2]^{1/2}$. Then we may construct a unit vector e from a vector y by $e = y/|y|$. Typically principal component analysis of many natural spectra shows that a single vector accounts for a major fraction of variability across many data sets. For example, three to five vectors are sufficient to explain almost all spectral variability in Landsat MSS and TM data for vegetated areas in the United States (Price, 1984). We may use the Gram–Schmidt procedure to obtain a set of spectral vectors representing the major variability of an ensemble of measurements. We begin by assuming a set of fitted measurement vectors δx^α of level K, which for $K = 0$ represent the difference from the mean of the data set $\langle x^\alpha \rangle$; $\delta x^\alpha = x^\alpha - \langle x \rangle$, and for $K > 0$ are given by $\delta x^\alpha = x^\alpha -$ (fit to level K), i.e., the result after reduction by fitting vectors to level K. We construct a basis set for the next iteration $K + 1$ by selecting vectors δx which are not described to within a norm of ϵ, i.e., $|\delta x| > \epsilon$, where the selection of ϵ will be described shortly. We begin the Gram–Schmidt procedure by averaging the first 10 spectra with $|\delta x| > \epsilon$, to construct a unit vector $e_1 = (\frac{1}{10}\Sigma \delta x)/|\frac{1}{10}\Sigma \delta x|$. The Gram–Schmidt method selects additional basis vectors after subtracting out the projection of those previously obtained. Thus after obtaining e_1, each measurement vector

δx is reduced to $\delta x' = \delta x - (e_1 \cdot \delta x)e_1$. This assures that $\delta x' \cdot e_1 = 0$. Then another 10 vectors $\delta x'$ with $|\delta x'| > \epsilon$ produce e_2, after which the reduced vector becomes $\delta x' = \delta x - (e_1 \cdot \delta x)e_1 - (e_2 \cdot \delta x)e_2$. Then $\delta x'$ after reduction by e_1 and e_2 is used to produce e_3, etc. By construction each Gram–Schmidt vector is orthogonal to all others: $e_i \cdot e_j = 0$ for $i \neq j$. In practice, the value ϵ must be selected so that the required number (also 10 in this analysis) of Gram–Schmidt vectors represents a sample throughout the entire ensemble of measurements. If ϵ is too large, then fewer than 10 Gram–Schmidt vectors result, whereas if ϵ is too small, only the early spectra in the data set are represented. The initial value of ϵ is found by trial and error for the data set in question, whereas later values are reduced as successive iterations produce better and better fits to the original spectra. At this point each spectrum may be represented, with a residual error, by the 10 Gram–Schmidt vectors, i.e., for all spectra $\delta x^\alpha = \sum c_i^\alpha e_i + r$, where the coefficients are given by $c_i^\alpha = (e_i \cdot \delta x^\alpha)$ and r is the residual.

Step 2. We now apply the principal components analysis to the covariance matrix formed from the 10 coefficients c_i representing the variability of the ensemble of δx^α. The inversion of a 10×10 matrix is straightforward. Then we use the resulting eigenvectors C_i to construct approximate eigenvectors $E_i = \sum_j C_{ij} e_j$ for the original data of dimensionality n. Thus the residual spectra δx^α at level K may now be expressed by $\delta x^\alpha \approx \sum_{i=1}^{10} c_i^\alpha E_i$, where $c_i^\alpha = E_i \cdot \delta x^\alpha$.

At this point a large fraction of the variability of the data set is accounted for in the 10 eigenvectors E_i. However, this description is not very useful. Each of the original basis vectors e_i is the mean of 10 individual spectra, and thus is subject to noise in these 10 measured spectra, so that the eigenvectors E are also noisy, i.e., they contain low amplitude high frequency variability. One may consider repeating the analysis, subtracting out the projections from the E_i already determined, and then finding an additional set for the residual vectors. However, this increases the number of basis vectors, which will eventually begin to approach the full spectral dimension n, and the later eigenvectors will show increasing effects of noise. For both reasons we seek to refine the analysis by using the spectral correlations implied in the eigenvectors E.

Step 3. There is a recognizable tendency for the majority of the variability of spectral data describing natural surfaces to be described by the first few eigenvectors E. Generally 60–90% are associated with the first eigenvector. Furthermore, the eigenvectors are found to be relatively smooth, i.e., they vary continuously and relatively slowly with wavelength. Since each eigenvector describes spectral behavior across the full spectral region, it is possible to select a broadband interval representing the spectral region where the eigenvector is large, and to use the spectral integral across this interval $S_i^\alpha = \int \delta x^\alpha \, d\lambda_i$ as a single parameter describing the total spectral behavior of the eigenvector, where we use the nomenclature for the integral

$$\int \psi \, d\lambda_i = \int_{\lambda_i(\min)}^{\lambda_i(\max)} \psi \, d\lambda .$$

This approach is approximate because the other (much smaller) eigenvectors also contribute to the broadband integral, in a statistical sense. Then we use the spectral integral to determine a wavelength-dependent fitting function F, which approximates the eigenvector explaining the largest amount of variability. Thus

$$\delta x^\alpha \approx F_i(\lambda) S_i^\alpha ,$$

where F is determined by a best fit across the data set, i.e.,

$$F_i(\lambda) = \langle \delta x^\alpha S_i^\alpha \rangle / \langle (S_i^\alpha)^2 \rangle .$$

It is appropriate to normalize F, i.e., we define

$$\varphi_i = F_i(\lambda) \Big/ \left[\int F_i(\lambda) \, d\lambda_i \right] \quad \text{so that } \int \varphi_i \, d\lambda_i = 1 .$$

Then each residual vector δx^α at iteration level K is approximated by $\delta x_K^\alpha \approx \varphi_K(\lambda) S_K^\alpha$, where $S_K^\alpha = \int \delta x^\alpha \, d\lambda_k$. At this point the original measurement vector may be reduced by this fitting function, and the process is repeated by going back to Step 1, where the number of fitting functions to be subtracted has increased by one. The advantages of this step (3) are: 1) Each fitting function φ results from the statistical fit to ALL the spectra, rather than being represented by the limited number accepted in the Gram–Schmidt procedure. 2) Each fitting function has as a coefficient a simple spectral integral, rather than the result of a vector inner product of the n-dimensional measured vector with the corresponding eigenvector E. Evi-

dently this step depends on selecting a spectral interval in which the major part of spectral variability is associated with the first eigenvector E, so that φ describes this first E well. This can only be determined in practice, but appears to work well for data sets examined. The procedure (Steps 1, 2, and 3) is terminated at level K when the residual vectors have no observable pattern, or seem to be dominated by noise, or when a single eigenvector from the principle components analysis no longer explains a major part of the spectral variability. In the example all three conditions appear simultaneously.

To this point we have been concerned only with spectral variability across the data set, after subtracting off the mean. In principle, the mean spectrum across an ensemble need not have the same properties as the variability about the mean. For example, the mean might contain a set of step functions with wavelength, while the variability varies smoothly with wavelength, or conversely. However, because both are the result of the physical property of reflectance, we expect them to represent the same spectral behavior, and to be described by the same fitting functions. Thus it should be possible to represent the spectral mean $\langle x(\lambda)\rangle$ by the fitting functions φ. We note, however, that this conclusion is not guaranteed: Instrumental biases can produce behavior in the mean which does not resemble the variability across the data set. The data set described in the next section does not suffer from this problem, and the mean is in fact described by the functions describing spectral variability, in the sense that amplitude of the ensemble mean $\langle x\rangle$ is well explained (98.6%) by the four spectral fitting functions which are found. As a result, the fitting functions to be presented next were obtained by completing the above analysis without subtracting off the mean. Thus for a measured spectrum x^α we conclude with the approximation at level K

$$x^\alpha(\text{level } K) = \sum_{i=1}^{K} \varphi_i(\lambda) S_i^\alpha,$$

where each S_i^α is the integral across the selected interval $(\lambda_i^{\min}, \lambda_i^{\max})$ of x^α less the previously determined fitting series, i.e.,

$$S_i^\alpha = \int d\lambda_i \left[x^\alpha - \sum_{j=1}^{i-1} \varphi_j(\lambda) S_j^\alpha \right].$$

We complete this section by observing that the integral of each integral $\int d\lambda_i \varphi_j$ over the φ may be computed at the beginning in order to simplify this formula.

It would appear that construction of the residual spectra would be required at each step in order to compute the integral for the coefficient of the next fitting function. This is not necessary, as the functions φ are known, having been derived in the analysis, so that their integrals are also known. Let

$$b_{ij} = \int \varphi_j \, d\lambda_i.$$

Thus b_{ij} is the integral over the ith spectral domain of the jth fitting function. Then it follows directly that given a spectrum x^α, we may construct the residual after the first fit using the integral $S_1^\alpha = \int x^\alpha \, d\lambda_1$ by

$$\delta x_1^\alpha = x^\alpha - S_1^\alpha \varphi_1,$$

which leads to the integral

$$S_2^\alpha = \int x^\alpha \, d\lambda_1 - S_1^\alpha \int \varphi_1 \, d\lambda_2 = \int x^\alpha \, d\lambda_2 - b_{21} S_1^\alpha,$$

etc., and only the set of spectral integrals over x is required. Thus we require only the set $s_i = \int x \, d\lambda_i$, and the precomputed values of b_{ij}. Define $S_1 = s_1$, and let

$$S_i = s_i - \sum_{j=1}^{i-1} b_{ij} S_j \quad \text{for } i > 1.$$

Then

$$x = \sum_{i=1}^{K} S_i \varphi_i,$$

where K is the total number of terms in the expansion, four in the case of the soils data.

APPLICATION TO SOILS DATA

The data used in this study represent an atlas of laboratory spectra measured at Purdue University (LARS). Excellent documentation (Stoner et al., 1980) is presented for the purpose and methodology of the collection of soil samples and their measurement as reflectance, that is, $x(\lambda) = L_{\text{reflected}} / L_{\text{incident}}$ (unitless). The majority of 564 samples were collected by the Soil Conservation Service of the USDA, while a few additional sam-

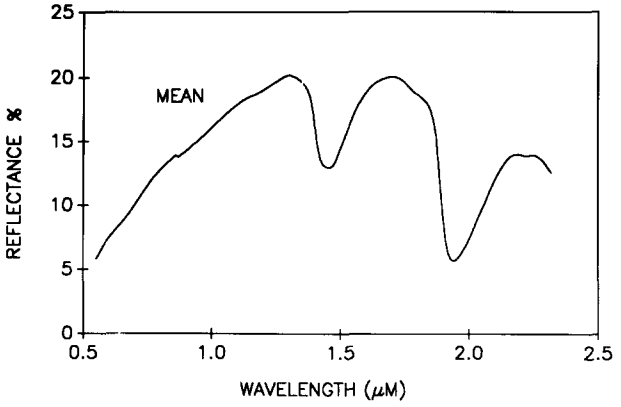

Figure 1. Mean reflectance for 564 soil reflectance spectra. The instrument uses two detectors, with the transition at about .85 μm.

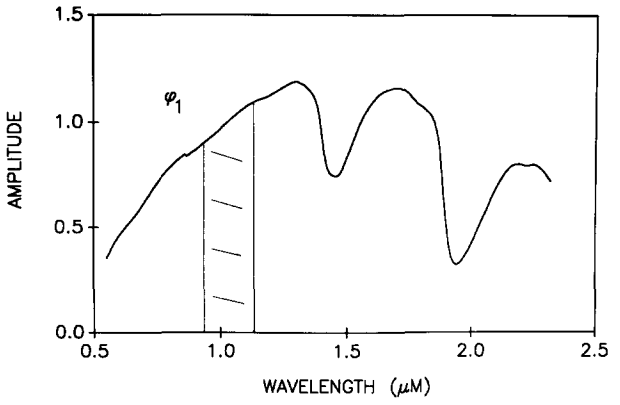

Figure 2. Amplitude values (unitless) for the first basis function, defined from the interval, .93–1.13 μm.

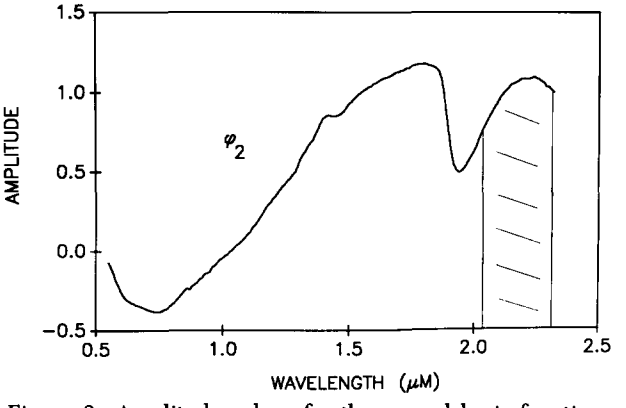

Figure 3. Amplitude values for the second basis function, defined for the interval 2.03–2.31 μm.

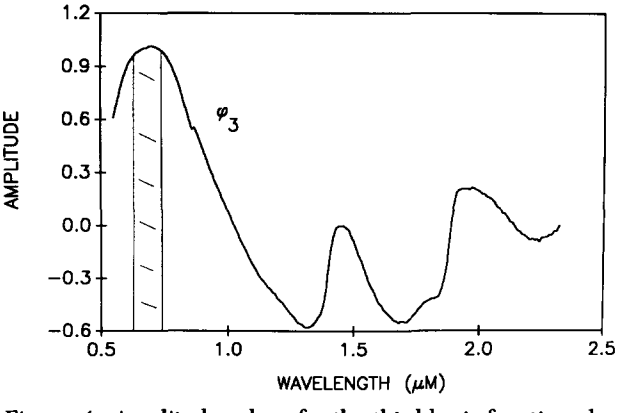

Figure 4. Amplitude values for the third basis function, defined for the interval .63–.74 μm.

ples were obtained from Brazil and other foreign countries. Measurements were made on moist soils at .1 bar tension. One soil, Fincastle silt loam, was measured a number of times as an indication of variability of the measurement process (Stoner et al., 1980, Fig. 5). No effort was made to eliminate these redundant spectra in this analysis. The data were acquired with an Exotech Model 20 radiometer, having a pass band of .55–2.32 μm. The data are available from Purdue University at a spectral sampling of .01 μm. The superior quality of the measurements is best indicated by the results of this analysis, with only the slightest indication of instrumental effects, and very low noise level. A detailed description of the instrumentation and measurement process may be found in Silva et al. (1971), Leamer et al. (1973), DeWitt and Robinson (1974), and Stoner (1979).

The mean of the 564 spectra is illustrated in Figure 1, while Figures 2–5 illustrate the spectral fitting functions and together with the associated spectral interval for spectral integration for establishing coefficients. The resemblance of the spectral mean of the data to the first fitting function describing variability suggests, as we would expect, that both result from the same physical properties of reflectance. By normalization, the integral of each fitting function across its corresponding spectral interval is 1. One may view the successive approximations of a spectrum x^{α} as the determination of coefficients (by integration) which force the residual to have zero mean value within the region of the integration. Thus the residual remaining after subtraction gets smaller and smaller as it is forced to zero at more and more locations across the full spectral domain.

We note a difference between laboratory spectra and remotely sensed spectra, i.e., measurements through an atmosphere. For the latter, atmospheric water vapor decreases the transmission

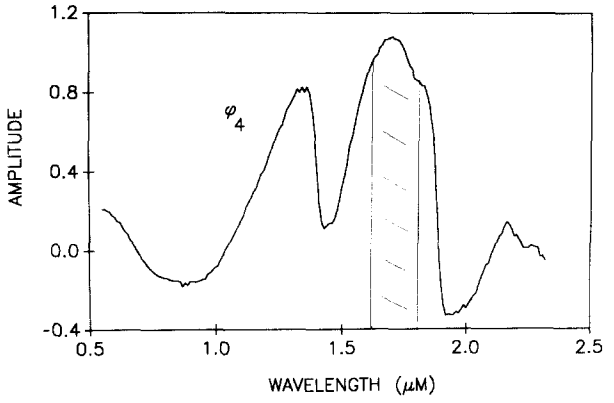

Figure 5. Amplitude values for the fourth basis function, defined for the interval 1.61–1.80 μm.

of radiation from the surface significantly in some spectral intervals. For this reason the spectral intervals 1.35–1.47 μm and 1.81–2.02 μm have been excluded during the selection of broadband intervals to represent the high resolution spectra. As a result, variability in these spectral intervals remain at the conclusion of the analysis, somewhat inflating the residual unexplained variance. This treatment is appropriate for remote sensing applications.

Table 1 presents quantitative information regarding the variability associated with successive levels of approximation. The columns have already been described except for the definition of the total variance in the data set, which is given by

$$\text{Variance}(K) = \sum_{\alpha=1}^{564} \sum_{i=1}^{178} \left[x_\alpha(\lambda_i) - \sum_{m=1}^{K} S_m \varphi_m \right]^2 .$$

Evidently the use of spectral integrals and the functions φ is slightly less efficient than the eigenvector analysis in describing variability at each step. Thus the variability associated with the first eigenvector at a given level of analysis, K, is somewhat greater than that eliminated by the resulting fitting function, e.g., the variance explained by the first fitting function (74.2%, the last entry in row 2) is less than the variance explained by the result of the first eigenvector analysis (87.9%, the value in row 1, column 3). However, each fitting function or basis function is noticeably smoother than the eigenvector which led to the selection of the corresponding interval of integration. Furthermore, evaluation of coefficients by spectral integration of x is simple and reduces noise, in the sense that integration is an averaging process, while the problems with the spectral eigenvectors have already been noted. In particular, evaluation of coefficients for spectral eigenvectors E requires construction of the inner product, i.e., computation on the entire spectral interval. It also precludes the use of an instrument acquiring a few broadband measurements, as is implied by the broadband integrals.

Although the rapid convergence of this procedure for the soils data set is evident, the identification of a concluding level of approximation is not necessarily clear. In the present case a number of factors point to the termination of the process. First, the dominant eigenvector after reduction of spectra by the first four basis functions contains only 43% of the residual variance (row 5, column 3), suggesting the presence of a mixture of uncorrelated effects such as noise. This contrasts with the identification of well-defined spectral absorption features which explain a major part of the residual variability for earlier steps in the iteration (column 3, rows 1–4). Secondly, the resulting eigenvectors after the fourth iteration (not shown) do not show large amplitude and smooth spectral behavior, in contrast to earlier cases. Additionally, trial selection of domains of integration for a hypothetical fifth basis function produces only a very minor reduction in variance, again contrary to earlier cases. Finally, the last residual spectral vectors appear to be very noisy, consistent with noise in the description of the instrumentation. Figure 6 illustrates the histogram of residuals for

Table 1

Fitting Value	*Wavelength Interval*	*% Variance in First Eigenvector*	*Unexplained Variance*	*Cum. % Variance Described*
0		87.9	32,891,000	—
1	.93–1.13	86.0	8,794,000	74.2
2	2.03–2.31	79.7	1,902,000	94.2
3	.63–.74	83.1	671,700	98.0
4	1.61–1.80	43.5	112,000	99.6

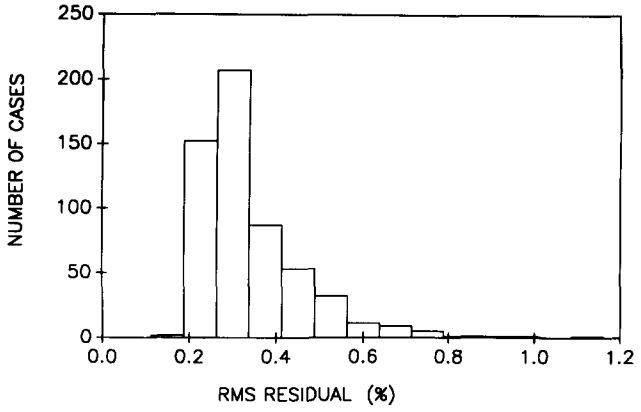

Figure 6. This histogram illustrates the number of spectra having a given root mean square residual. The worst fit spectra (Figures 7–10) fall at the extreme right (> 1%).

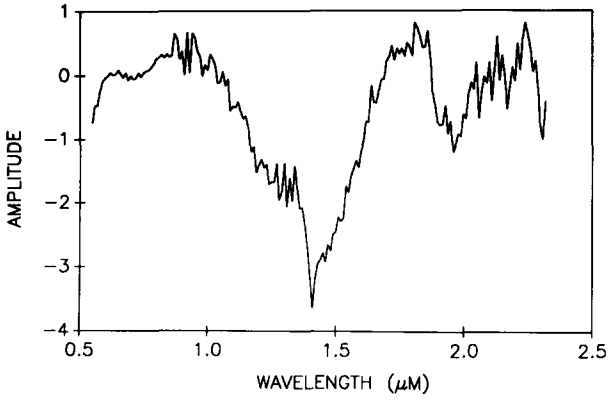

Figure 7. Deviation of the fitted spectrum from the best fit (%), worst case among 564 samples.

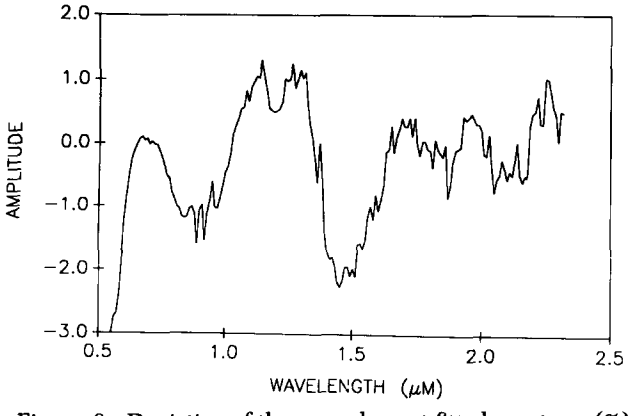

Figure 8. Deviation of the second worst fitted spectrum (%).

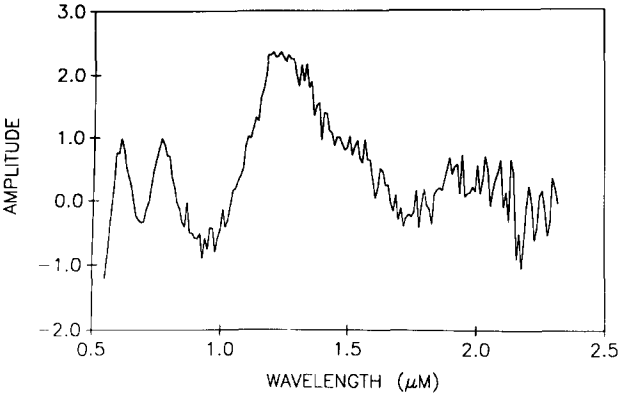

Figure 9. Deviation of the third worst fitted spectrum (%).

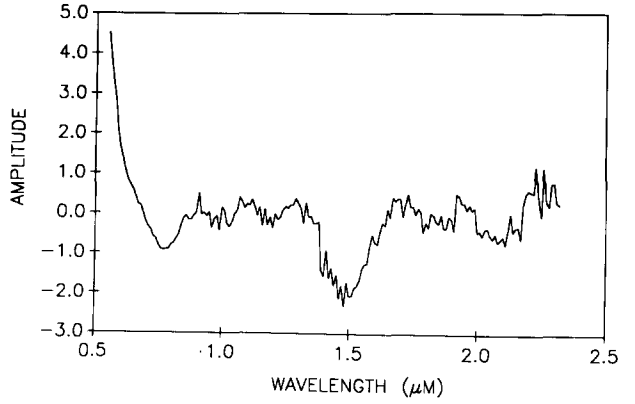

Figure 10. Deviation of the fourth worst fitted spectrum (%).

the spectral data set, and Figures 7–10 illustrate the residuals for four spectra (from 564) having the greatest norm, i.e., those illustrating the poorest fit. At this point further statistical processing is not warranted. One may consider identifying as special cases these spectra with largest residuals and cataloging them. However, it would be desirable to repeat the measurements of these spectra, in order to verify the reproducibility of these measurements. In addition, measurement of alternate samples of these soils would be desirable. It is not clear that these residual spectral effects are significant in the remote sensing context, where large areas are to be studied.

It is not appropriate to list here the 564 soils and their respective amplitudes S_i. Values for any soil may be obtained by appropriate integration of measured spectra, and the basis functions in Figures 2–5 permit the reconstruction of high resolution data from four broad band measurements. Of course, it has not been shown that U.S. soils provide an adequate representation of the world's soils. The author would appreciate receiving information on other soil groups.

One question which may be addressed is the tendency for clustering in the soil reflectance data. To what extent do soil reflectances fall into groups?

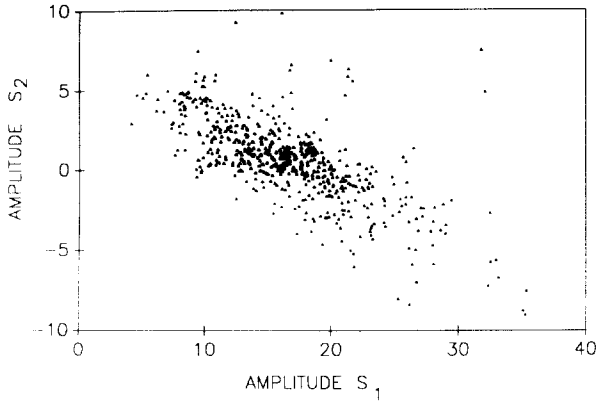

Figure 11. The scattergram illustrates the variability of the second integral versus the first integral. Points at the lower left are excluded because reflectances are always positive.

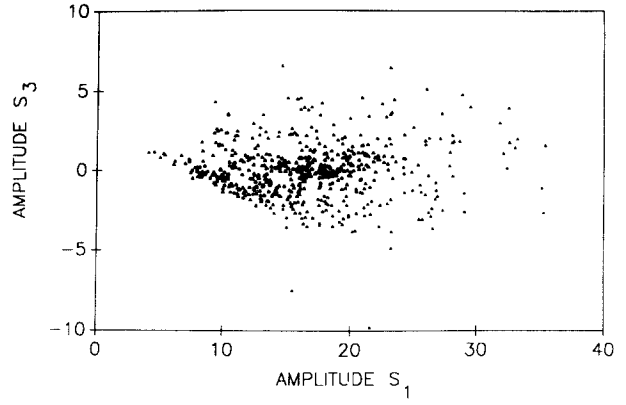

Figure 12. The scattergram illustrates the variability of the third integral versus the first.

This question may be addressed by plotting the scattergram of values of the S_i, $i > 1$, versus the distribution of the first integral, S_1. These results are presented in Figures 11–13. We point out the decrease in the amplitude of successive coefficients S_2, S_3, S_4. Evidently no significant clustering exists among reflectance values for the U.S. soils data, although there is an apparent correlation between S_1 and S_2 values which is cancelled by the effect of a small number of outliers.

Finally, we consider the method for handling broadband measurements in intervals other than those recommended. Evidently the φ functions may be used to derive by integration the results of other selections of spectral bands, such as in the Landsat instruments. Although such measurements would be less than optimum compared to those selected here, in the sense of instrument

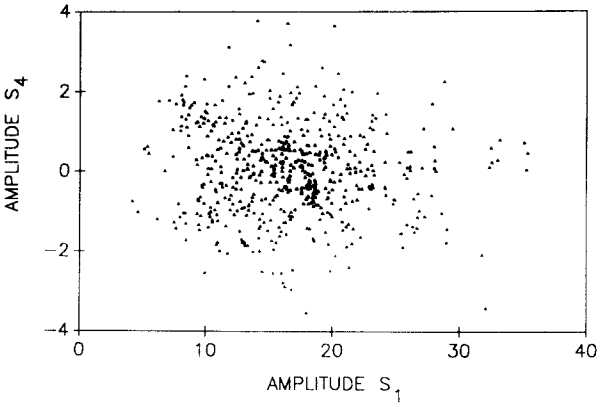

Figure 13. The scattergram illustrates the variability of the fourth integral versus the first.

signal to noise ratio, they, together with the φ functions, would also describe the high resolution spectra fully, provided only that the measurements are statistically independent of each other.

CONCLUSION

A procedure developed for identifying independent spectral variability in the thermal infrared has been applied to visible-near infrared spectra from a data base of U.S. soils. Although thermal infrared spectra from satellite height contain numerous sharp spectral features associated with molecular absorption and emission in the earth's atmosphere, reflectance spectra for soils are characterized by broad smooth features. Thus identification of the spectral intervals chosen for soil characterization (.93–1.13 μm, 2.03–2.31 μm, .63–.74 μm, 1.61–1.80 μm) with specific soil/chemical properties does not appear to be possible, in contrast with the thermal infrared study (Price, 1975, Table 1). This is unimportant, as there appears to be no quantitative theory for spectra of solid materials such as soils in the visible and near infrared, and chemical composition is not generally specified in soils specification. In contrast, thermal infrared spectra are known for most molecules in the atmosphere. Evidently it would be desirable to apply the procedure to vegetation and to geologic spectra. Both soil and atmospheric spectral analyses show the possibility of describing high spectral resolution data with only a few relatively broad band measurements.

Thus 862 spectral values may be described by nine basis functions, in the case of atmospheric spectra, while 178 measurements may be described by four basis functions, in the case of soil spectra. This result suggests the use of relatively simple instrumentation and data processing systems for inferring soils information from remotely sensed data, assuming that field reflectances are represented adequately by the laboratory data. Finally, as a not insignificant conclusion, we relate these findings to the use of the Munsell color system by the Soil Conservation Service (SCS) of the USDA for describing soil color. The Munsell system (Munsell Color, 1988) consists of matching soil samples to color patches in a field handbook for hue, value, and chroma, or hue, intensity, and saturation in the modern nomenclature. The human visual system relies on discrimination of these three color variables, and Munsell soil charts illustrate samples with three variables. This analysis shows that four spectral measurements are sufficient to describe visible/near infrared variability, although the blue portion of the spectrum is missing from the data studied. Barring unexpected variability in the blue portion of soil reflectance, it appears that the semiquantitative method used by SCS is capable of discriminating the major part of spectral variability of U.S. soils.

REFERENCES

Dewitt, D. P., and Robinson, B. F. (1974), Description and evaluation of a bidirectional reflectance reflectometer, LARS Information Note 091576, Laboratory for Applications of Remote Sensing, Purdue University, West Lafayette, IN.

Leamer, R. W., Meyers, V. I., and Silva, L. F. (1973), A spectroradiometer for field use, *Rev. Sci. Instrum.* 44:611–614.

Munsell Color (1988), Munsell Soil Color Charts and Determination of Soil Color, from U.S.D.A. Handbook 18—Soil Survey Manual, Kollmorgen Instruments Corp., Baltimore, MD.

Price, J. C. (1975), Information content of IRIS spectra, *J. Geophys. Res.* 80:1930–1936.

Price, J. C. (1984), Comparison of the information content of data from the Landsat 4 Thematic Mapper and the Multispectral Scanner, *IEEE Trans. Geosci. Remote Sens.* GE-22:272–281.

Silva, L. F., Hoffer, R. M., and Cipra, J. E. (1971), Extended wavelength field spectroradiometry, in *Proc. 7th Int. Symp. on Remote Sensing of Environment*, Ann Arbor, MI, Vol. II, pp. 1509–1518.

Stoner, E. R. (1979), An approach toward a rational classification of climate, *Geograph. Rev.* 38:55–94.

Stoner, E. R., Baumgardner, M. F., Biehl, L. L., and Robinson, B. F. (1980), Atlas of Soil Reflectance Properties, Research Bulletin 962, Purdue University, West Lafayette, IN.